SCIENTIFIC REPORTS

OPEN

SUBJECT AREAS:
NEUROGENIC BLADDER
MECHANISMS OF DISEASE
MULTIPLE SCLEROSIS
PHYSIOLOGY

Received
5 March 2013

Accepted
20 June 2013

Published
5 July 2013

Correspondence and requests for materials should be addressed to S.O.S. (sylvia.suadicani@einstein.yu.edu)

Pannexin 1 involvement in bladder dysfunction in a multiple sclerosis model

Hiromitsu Negoro[1], Sarah E. Lutz[2], Louis S. Liou[3], Akihiro Kanematsu[4,5], Osamu Ogawa[4], Eliana Scemes[2] & Sylvia O. Suadicani[1,2]

[1]Department of Urology, [2]Dominick P. Purpura Department of Neuroscience, Albert Einstein College of Medicine, Bronx, NY, 10461, USA, [3]Department of Urology, Cambridge Health Alliance, Cambridge, MA, 02139, USA, [4]Department of Urology, Graduate School of Medicine, Kyoto University, Sakyo, Kyoto 606-8507, Japan, [5]Department of Urology, Hyogo College of Medicine, Nishinomiya, Hyogo 663-8501, Japan.

Bladder dysfunction is common in Multiple Sclerosis (MS) but little is known of its pathophysiology. We show that mice with experimental autoimmune encephalomyelitis (EAE), a MS model, have micturition dysfunction and altered expression of genes associated with bladder mechanosensory, transduction and signaling systems including *pannexin 1* (*Panx1*) and *Gja1* (encoding connexin43, referred to here as *Cx43*). EAE mice with *Panx1* depletion ($Panx1^{-/-}$) displayed similar neurological deficits but lesser micturition dysfunction compared to $Panx1^{+/+}$ EAE. *Cx43* and *IL-1β* upregulation in $Panx1^{+/+}$ EAE bladder mucosa was not observed in $Panx1^{-/-}$ EAE. In urothelial cells, IL-1β stimulation increased Cx43 expression, dye-coupling, and p38 MAPK phosphorylation but not ERK1/2 phosphorylation. SB203580 (p38 MAPK inhibitor) prevented IL-1β-induced Cx43 upregulation. IL-1β also increased *IL-1β*, *IL-1R-1*, *PANX1* and *CASP1* expression. Mefloquine (Panx1 blocker) reduced these IL-1β responses. We propose that Panx1 signaling provides a positive feedback loop for inflammatory responses involved in bladder dysfunction in MS.

Multiple sclerosis (MS) is a degenerative autoimmune demyelinating disease that affects the brain and spinal cord. The onset of MS ranges from 20 to 40 years of age, with more than 80% of MS patients suffering from bladder symptoms, such as urgency, urinary incontinence, nocturia, and urinary retention[1,2].

Experimental autoimmune encephalomyelitis (EAE) is one of the most commonly used and characterized animal model of MS[3]. Similar to what is observed in humans with MS, rodents with EAE present CNS lesions with inflammation, demyelination, axonal loss and gliosis[4], and display significant bladder dysfunction[5–9]. In mice with EAE, significant increase in bladder size[5], increase in micturition frequency, decrease in urine volume voided per micturition (UVVM), changes in morphology[6] and expression of molecular markers of fibrosis among others[7], have been observed with progression of the disease and increase in neurological deficit. In rats with EAE, cystometric analysis showed changes in detrusor activity, such as detrusor hyperreflexia (bladder overactivity) and detrusor areflexia[8,9], which closely resemble urodynamic changes observed in MS patients[10], and have been attributed to an imbalance between the inhibitory and excitatory stimulation within the spinal cord centers controlling the micturition reflex[8]. These findings are in line with the current view that bladder dysfunction in MS results mostly from spinal cord demyelination and consequent disruption of pathways between the lumbosacral region and pontine micturition center that coordinate the activity of the bladder detrusor and urethral sphincter muscles.

Besides CNS control of bladder function, there are other regulatory systems intrinsic to the bladder, which play key roles in the control of urination[11,12]. Components of these systems include the ones involved in the perception and transduction of bladder distention, essential for proper activation of the micturition reflex, and others mediating the transmission of signals within the bladder wall which contribute to modulation of detrusor muscle function. Moreover, in response to various pathological conditions, such as bacterial infection and bladder outlet obstruction, the bladder produces cytokines, chemokines and growth factors, and undergoes remodeling of its tissue components[13–15]. In addition, abnormal bladder distention or high pressure voiding due to neurological deficit in neurogenic bladder also triggers significant bladder remodelling, which may also involve expression of inflammatory mediators[16]. These responses induce bladder symptoms, such as frequency and urgency[17–19], and contribute to further bladder dysfunction[12,20]. However, little is still known of the importance of these bladder

responses and of changes in bladder intrinsic regulatory systems to bladder dysfunction in MS, which is primarily viewed as neurogenic in etiology.

Molecular changes in the bladder have been investigated in various pathological conditions in humans and animals[20]. Among them, genes associated with bladder mechanosensory, transduction and signaling systems have been recently highlighted and found to have important roles in bladder remodeling, such as purinergic receptors[21], cholinergic receptors[22], transient receptor potential cation channels (TRP)[23], connexins[24] and others. Pannexin 1 (Panx1), a member of the gap junction family of proteins that forms non-junctional channels[25], could likely be included in this list. In contrast with connexins, Panx1 forms large channels that are not only voltage but also mechanosensitive, allowing the diffusion of ions and signaling molecules (up to 1,500 Da) between the cytoplasm and the extracellular space. Panx1 is expressed in various cell types and participates in key cellular events, such as intercellular and mechanotransduction signaling, and in inflammatory responses[26–28].

Here we show that expression of certain genes associated with the bladder mechanosensory, transduction and signaling systems was altered in mice with EAE and that genetic depletion of *Panx1* ameliorated micturition function and prevented the associated upregulation of the gene *Gja1* (encoding connexin 43; a gap junction protein, and referred to here as *Cx43*) and *interleukin 1 beta* (*IL-1β*; a pro-inflammatory cytokine) in the bladder mucosa of EAE mice. Furthermore, based on our *in vitro* studies with a human urothelial cell line exposed to IL-1β, we propose that a positive feedback mechanism between Panx1 and IL-1β via IL-1β receptor type 1 (IL-1R-1) contributes to bladder dysfunction as seen in mice with EAE. In this mechanism, activation of IL-1R-1 upregulates *Cx43* and *IL-1β* via a p38 MAPK pathway and, through a yet unknown pathway, also increases *Panx1* expression. In turn, Panx1 signaling would feedback by promoting caspase-1 (Casp1, IL-1β converting enzyme) activation.

Results

Micturition dysfunction in EAE mice. In this study we used the aVSOP (automated Voided Stain on Paper), a method that we have shown to assess mouse micturition in a more accurate manner[29,30], particularly in cases when UVVM are less than 50 µl, as observed in mice with EAE, which is difficult to be measured using electronic balance systems. One week after immunization, C57BL/6 mice started displaying neurological deficits which progressed from flaccid tail to hindlimb paralysis at 20 days post immunization (dpi); this initial phase of the disease is referred to here as the acute phase. The acute phase was then followed by a stable phase with minimal recovery, referred to as the chronic phase (Figure 1A). Micturition dysfunction was not obvious in the acute phase, but was evident in the chronic phase and characterized by a significant decrease in UVVM (Figure 1B and C). Increase in bladder weight was also apparent in the chronic phase (Figure 1D). These findings suggest that in the acute phase even at high neurological deficits, bladder dysfunction may still be mild and undetectable, but as the disease progresses through the chronic phase, bladder alterations are no longer compensated for.

Panx1 and Cx43 expression are increased in bladder mucosa of EAE mice. Bladder mucosa and detrusor muscle of naïve and EAE mice were separated and changes in expression of genes associated with the bladder mechanosensory, transduction and signaling systems were quantified in each compartment. Validation of proper compartment separation was determined by real-time PCR, showing enrichment in the mucosa of mRNA for the markers *Cdh1* (known as *E-cadherin*) and *Upk3a* (*uroplakin 3a*), and in the detrusor for the marker *Des* (*Desmin*) (Supplementary Fig. S1). We next focused on *Panx1*, *Cx43*, *P2rx (purinergic P2X receptor)*, *P2ry (purinergic P2Y receptor)* and other transcripts of genes known to be associated with the bladder mechanosensory, transduction and signaling systems, and compared their expression levels in bladders of control mice (naïve) and in mice with EAE (acute and chronic phases). We found in the mucosa that *Panx1*, *Cx43*, *P2rx3*, *P2ry1*, *Trpv4* (*transient receptor potential cation channel, subfamily V, member 4*) and *Chrm2* (*cholinergic receptor, muscarinic type 2*) transcripts were significantly upregulated, while urothelial marker genes such as *Cdh1, Upk1a* and *Upk3a* were not altered (Figure 2A, B and Supplementary Fig. S2). Confirmation of increased Panx1 and Cx43 protein levels was obtained by immunoblotting in the chronic phase of EAE (Figures 2C and D). Specificity of bands for Panx1 was verified using naive $Panx1^{+/+}$, $Panx1^{+/-}$ and $Panx1^{-/-}$ mice (Figure 2C). In non-EAE, CFA-only treated mice, *Panx1* and *Cx43* mRNA expression levels as well as bladder weight and UVVM were not significantly different from control (naïve) mice at the same time

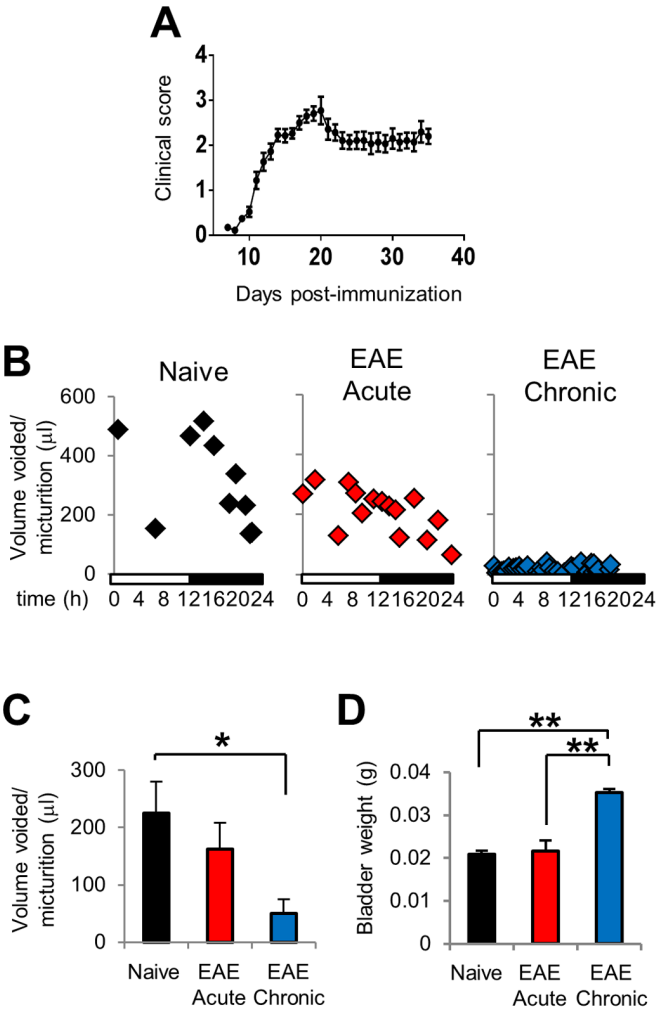

Figure 1 | Micturition dysfunction in C57BL/6 wild type mice with EAE. (A) Time course of neurological symptoms in mice with EAE (n = 28, 5 mice died at dpi 10, 11, 15, 16 and 21). (B, C) Representative charts of UVVM of naïve mice (left), EAE mice in acute phase (16–17 dpi, middle) and EAE mice in chronic phase (38–39 dpi, right) in (B), and average UVVM in (C). EAE mice in chronic phase had significantly lower functional bladder capacity than naïve mice. $*P < 0.05$ by Kruskal Wallis test followed by Dunn's *post-hoc* test (n = 4, 3 and 6, respectively). (C) Bladder weight was significantly increased in chronic phase. $**P < 0.01$ by one-way ANOVA followed by Tukey's *post-hoc* test (n = 6, 7 and 5, in naïve, acute and chronic phases of EAE, respectively). All error bars represent SEM.

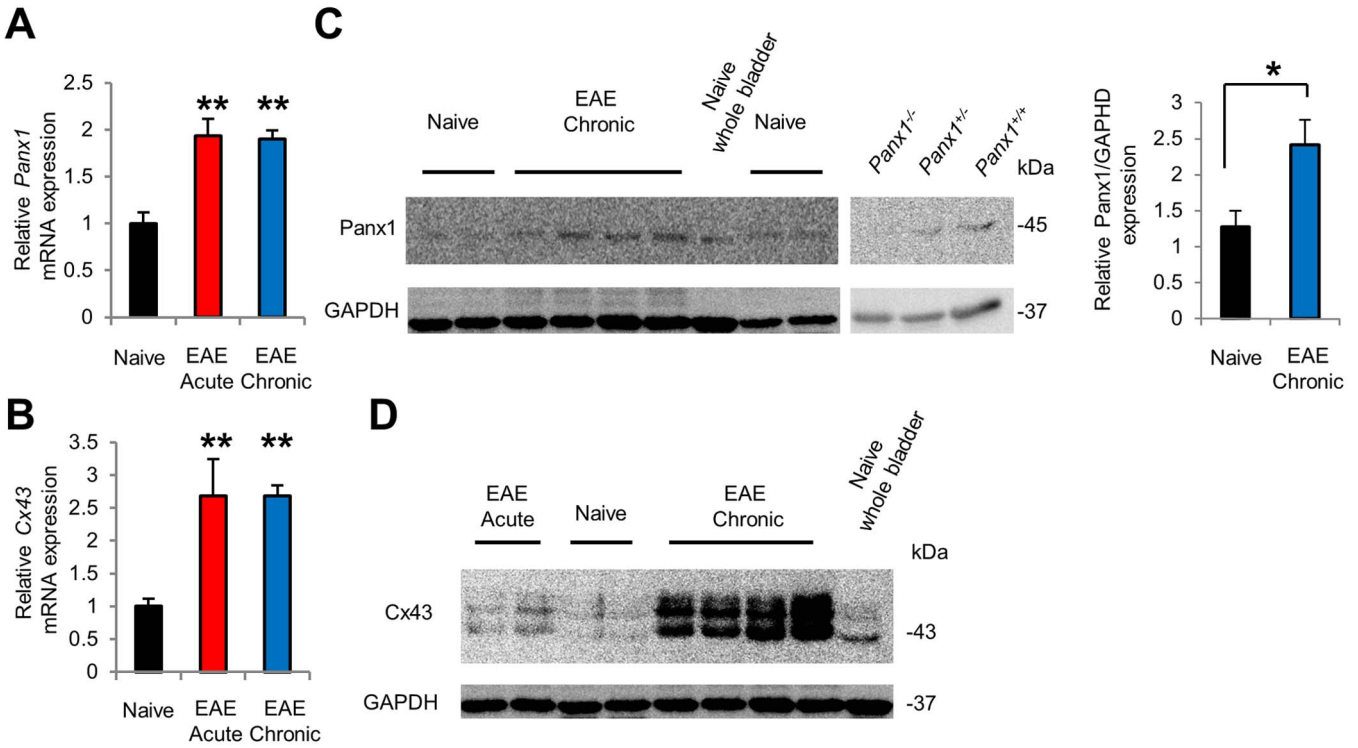

Figure 2 | EAE mice display increased Panx1 and Cx43 expression levels in bladder mucosa. (A, B) Increased *Panx1* mRNA expression in (A) *Cx43* mRNA expression in (B) in mucosa of EAE mice in acute and chronic phases (n = 5, 3 and 3 in naïve, EAE acute phase and EAE chronic phase, respectively). $^{**}P < 0.01$ by one-way ANOVA followed by Tukey's *post hoc* test. (C) Blot on the left: Increased Panx1 protein expression in chronic phase. $^{*}P < 0.05$ by unpaired *t*-test (n = 4). Blot on the right: Specificity of the Panx1 antibody is demonstrated by the absence of the expected band in the protein homogenate of $Panx1^{-/-}$ mouse bladder. (D) Increased Cx43 protein expression in chronic phase. All error bars represent SEM. For the relative levels, the values from naïve mice were set as 1 in (A) and (B), and the value of naïve bladder was set as 1 in (C). Full-length blots are presented in Supplementary Fig. S11.

points corresponding to the acute and chronic phases of EAE (Supplementary Fig. S3). In the detrusor, *Panx1*, *P2rx3*, *P2ry1*, *P2ry2*, *P2ry6* and *Chrm2* transcripts were found to be upregulated while the *P2rx1*, a major purinergic receptor in this compartment, was found to be downregulated (Supplementary Fig. S4). Genes associated with fibrosis such as *Col1a1* (*collagen, type 1, alpha 1*) and *Ctgf1* (*connective tissue growth factor*) were also upregulated in chronic EAE, findings that are consistent with a previous report[7]. The muscle marker *Des* was stable, similar to what was observed for the mucosa markers (Supplementary Figs. S2 and S4). These findings indicating remarkable changes in expression levels of genes associated with the mechanosensory, transduction and signaling systems in the bladders of mice with EAE suggest that these genes are likely involved in development of micturition dysfunction observed in EAE.

Because there is emerging evidence that Panx1 is related to various pathophysiological conditions, such as seizure[31], death of enteric neurons during colitis[27], nonalcoholic steatohepatitis[32] and others, and because Cx43 has been reported to have important roles in bladder function[17,18,24,29,33], we focused our study on these two gap junction genes, *Panx1* and *Cx43*. When comparing *Panx1* and *Cx43* expression in the bladder mucosa and detrusor compartments, we found that *Panx1* mRNA was mainly expressed in mucosa while *Cx43* mRNA was found in both mucosa and detrusor (Supplementary Fig. S5).

Genetic depletion of *Panx1* ameliorates micturition and prevents upregulation of Cx43 in EAE mice. To investigate the contribution of Panx1 in bladder dysfunction in EAE mice, we used $Panx1^{-/-}$ mice and compared the bladder phenotype of $Panx1^{-/-}$ EAE with that of $Panx1^{+/+}$ EAE mice in the chronic phase. Clinical scores of these two genotypes were not different in the chronic phase of EAE (Figure 3A), but micturition function in $Panx1^{-/-}$ EAE mice was significantly better than in $Panx1^{+/+}$ EAE mice; this was evidenced by the significantly higher UVVM (Figure 3B) and lower bladder weight of $Panx1^{-/-}$ EAE mice (Figure 3C) at 35–41 dpi when compared to those of $Panx1^{+/+}$ EAE mice. Moreover, absence of Panx1 prevented the upregulation of *Cx43* mRNA and its protein in the bladder mucosa seen in $Panx1^{+/+}$ EAE mice (Figures 3D and E). On the other hand, upregulation of *P2ry1* and *Chrm2* in the mucosa, and upregulation of *P2ry2* and *P2ry6* and downregulation of *P2rx1* in the detrusor was observed in both $Panx1^{+/+}$ EAE and $Panx1^{-/-}$ EAE mice (Supplementary Fig. S6). No significant differences in these parameters were observed between $Panx1^{+/+}$ naïve and $Panx1^{-/-}$ naïve mice (Supplementary Fig. S7), which supports the hypothesis that depletion of Panx1 contributed to the amelioration of bladder function in EAE.

Our findings that depletion of Panx1 prevented upregulation of Cx43 expression in the bladder mucosa of EAE mice (Figure 3D and E) is quite intriguing and suggest a correlation between Panx1 and Cx43 expression, at least in the bladder mucosa. Cx43 expression in the mouse bladder mucosa was further demonstrated by immunostaining (Figure 3F), which was more pronounced in the EAE mice urothelium. Specificity of Cx43 immunoreactivity was verified in urothelium explants cultured from $Cx43^{+/+}$, $Cx43^{+/-}$ and $Cx43^{-/-}$ mice (Figure 3G). It is likely, therefore, that Panx1 contribution to micturition dysfunction in EAE mice involves a mechanism that links Panx1 and Cx43 expression in the urothelium.

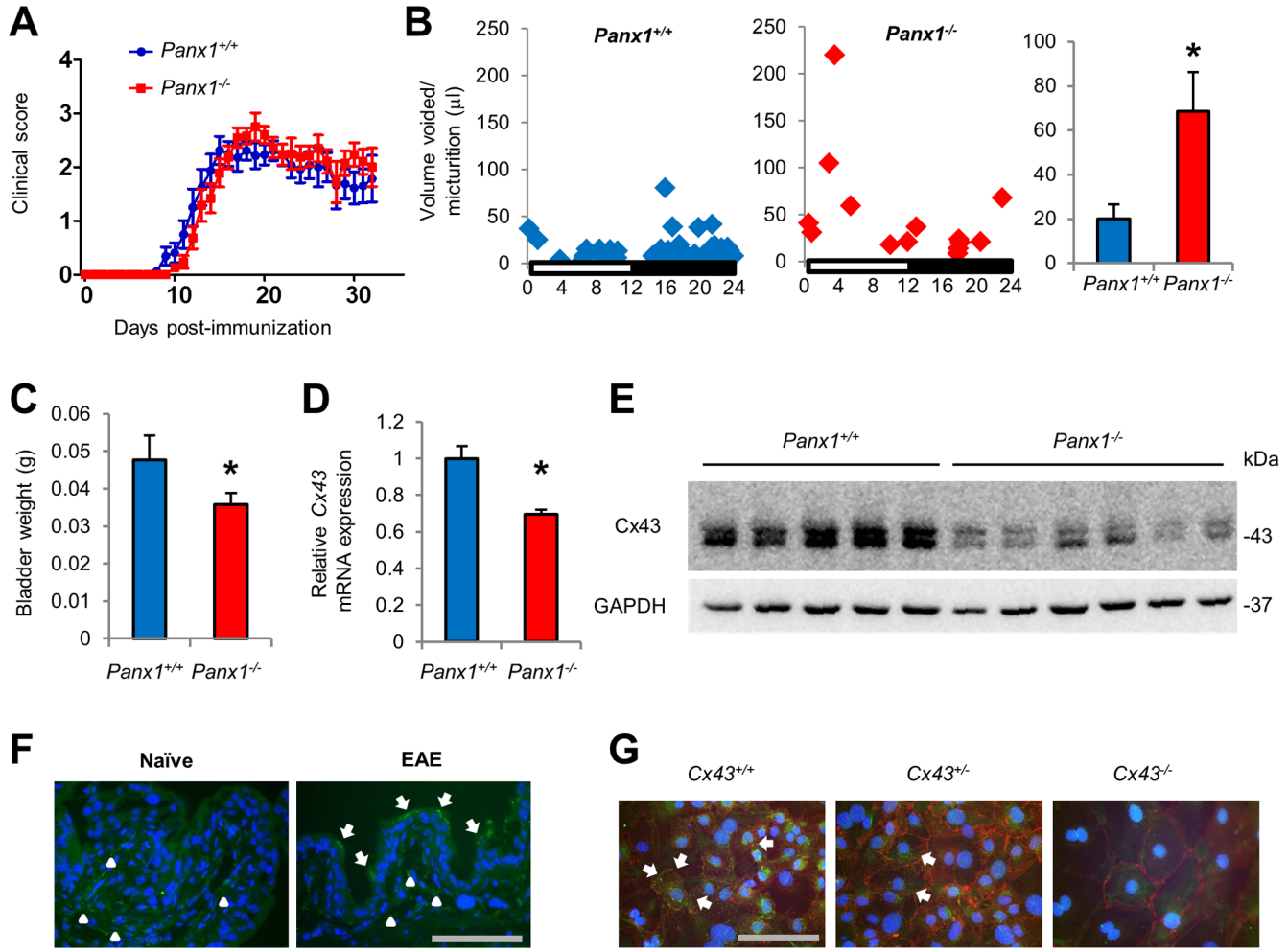

Figure 3 | Genetic depletion of *Panx1* ameliorates bladder dysfunction and prevents Cx43 upregulation in EAE mice. (A) Clinical score of $Panx1^{+/+}$ EAE and $Panx1^{-/-}$ EAE mice (n = 16, $Panx1^{+/+}$; n = 19, $Panx1^{-/-}$; Three $Panx1^{+/+}$ mice died). No significant difference in neurological deficits, as determined by two-way repeated measures ANOVA (Three dead $Panx1^{+/+}$ mice were excluded from the ANOVA, but an analysis before deaths was also not significant). (B) Representative charts for UVVM of $Panx1^{+/+}$ EAE mice [left, Clinical Score (CS) = 2], $Panx1^{-/-}$ EAE mice (middle, CS = 3), and average UVVM (right). $Panx1^{-/-}$ EAE mice in chronic phase had significantly higher UVVM than $Panx1^{+/+}$ EAE mice. $^*P < 0.05$ by Mann-Whitney U test (n = 3, $Panx1^{+/+}$; n = 8, $Panx1^{-/-}$). (C) Bladder weight of $Panx1^{-/-}$ EAE was significantly lower than that of $Panx1^{+/+}$ EAE mice. $^*P < 0.05$ by unpaired *t*-test. (n = 8, $Panx1^{+/+}$; n = 14, $Panx1^{-/-}$). (D, E) Cx43 expression in the bladder mucosa of $Panx1^{-/-}$ EAE was lower than that in $Panx1^{+/+}$ EAE mice; mRNA is shown in (D) and protein in (E) (full-length blots are presented in Supplementary Fig. S12). $^*P < 0.05$ by unpaired *t*-test. (n = 3, $Panx1^{+/+}$; n = 8, $Panx1^{-/-}$ in (D)). (F) Representative immunostaining of Cx43 in the bladders of $Panx1^{+/+}$ naïve and EAE mice. Arrows indicate positive staining in urothelium, more evident in EAE mice, and arrow heads in submucosa. Scale bar = 100 µm. (G) Cx43 immunostaining in urothelial cells cultured from $Cx43^{+/+}$, $Cx43^{+/-}$ and $Cx43^{-/-}$ mice. Green, Cx43; Red, E-cadherin. Arrows indicate typical dot stain of gap junctions. Scale bar = 100 µm. All error bars indicate SEM.

IL-1β is upregulated in $Panx1^{+/+}$ EAE but not in $Panx1^{-/-}$ EAE mice, and IL-1β increases Cx43 expression and function in cultured urothelial cells. Previous studies indicated that Panx1 is critical for the processing and release of IL-1β by activating the inflammasome[26,34]. In addition, IL-1β has been shown to upregulate Cx43 expression in various cell types[35,36], which prompted us to investigate whether mRNA expression levels of *IL-1β* and of its functional receptor *IL-1R-1* were altered in mice with EAE. We observed that in bladder mucosa the *IL-1β* and *IL-1R-1* mRNA levels were increased in EAE mice (Figure 4A and Supplementary Fig. S8). Notably, in mucosa of $Panx1^{-/-}$ EAE mice this upregulation of *IL-1β* expression was not observed and the upregulation of *IL-1R-1* was significantly lower than in their $Panx1^{+/+}$ EAE counterparts (Figure 4A).

To investigate whether changes in IL-1β signaling pathway were related to increased Cx43 expression levels as seen in EAE, we used a hTERT-immortalized non-transformed human urothelial cell line (TRT-HU1)[37] and studied its response to IL-1β. Stimulation of TRT-HU1 cells with IL-1β for 48 h significantly increased the expression levels of *Cx43* mRNA and its protein (Figures 4B and C). To determine whether these higher levels of *Cx43* mRNA and its protein were accompanied by increased Cx43-mediated gap junctional communication, we performed the Lucifer yellow dye-transfer assay in TRT-HU1 cells. The number of cells to which the dye spread was significantly higher in IL-1β treated compared to non-treated cells (Figure 4D).

IL-1β signaling via p38 MAPK. To identify the IL-1β signaling pathway involved in Cx43 upregulation, we evaluated the activation of two downstream kinases, p38 MAPK and ERK[38], known regulators of Cx43[18,39], and also the activation of STAT1, which is induced by IL-1β stimulation[40,41]. Stimulation of TRT-HU1 cells with IL-1β caused an increase in p38 MAPK and STAT1 phosphorylation but not in ERK phosphorylation (Figure 5A). Inhibition of p38

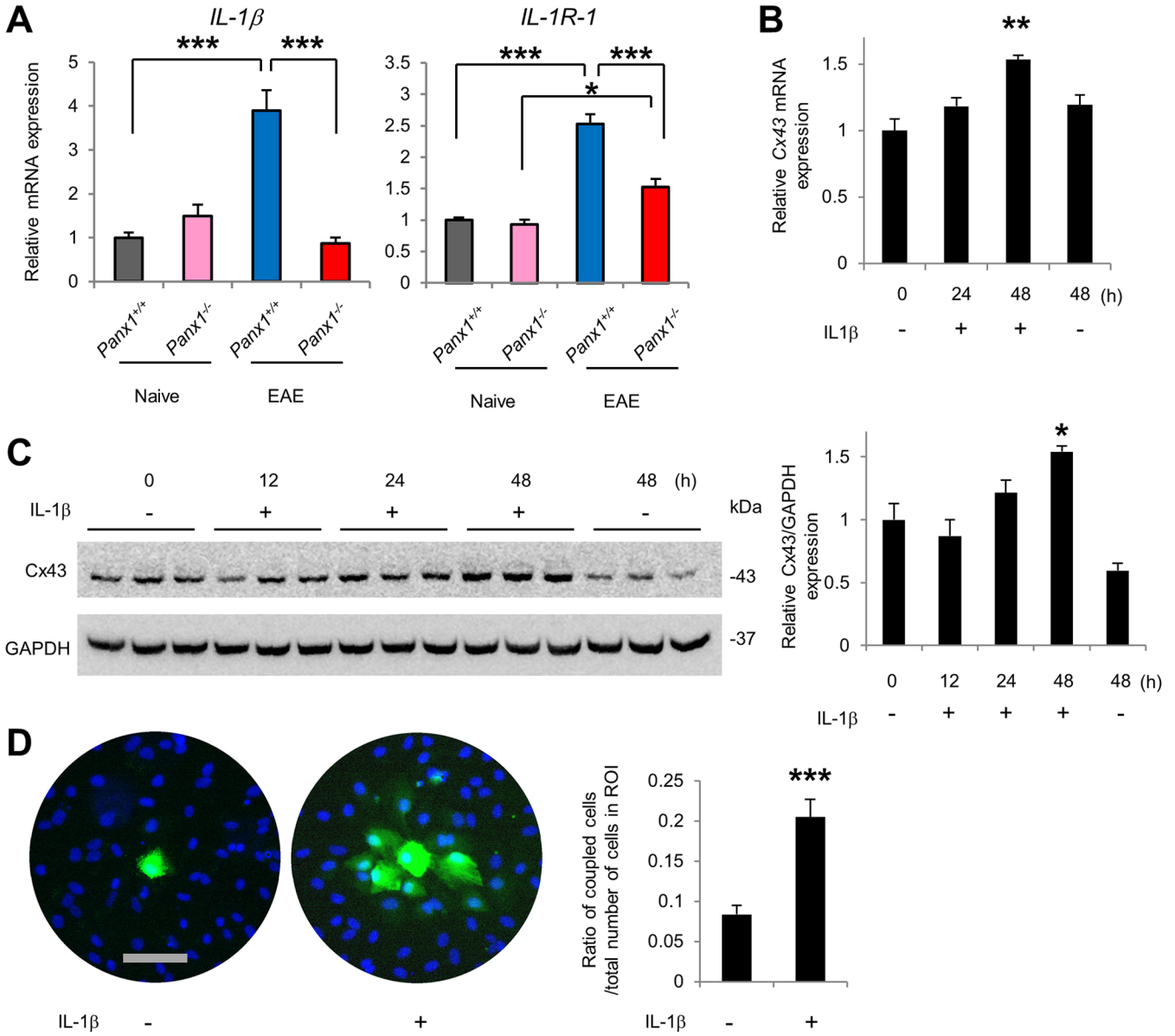

Figure 4 | IL-1β is upregulated in *Panx1*$^{+/+}$ but not in *Panx1*$^{-/-}$ EAE mice, and IL-1β increases Cx43 expression and function in cultured urothelial cells. (A) *IL-1β* mRNA expression in bladder mucosa of *Panx1*$^{+/+}$ EAE mice was significantly increased when compared to that in naïve *Panx1*$^{+/+}$ mice mucosa, a phenomenon that was not observed in *Panx1*$^{-/-}$ EAE mice. *IL-1R-1* upregulation in *Panx1*$^{-/-}$ EAE mice was significantly lower than in *Panx1*$^{+/+}$ EAE mice. *** $P < 0.001$ and * $P < 0.05$ by one-way ANOVA followed by Bonferroni's *post hoc* test (n = 5, 4, 3 and 8, respectively). (B, C) IL-1β stimulation of TRT-HU1 cells increased levels of *Cx43* mRNA in (B) and its protein in (C) (full-length blots are presented in Supplementary Fig. S13) (n = 3 for each time). * $P < 0.05$ and ** $P < 0.01$ compared with time 0 h and 48 h without IL-1β stimulation using one-way ANOVA followed by Tukey's *post hoc* test. (D) Enhanced gap junctional communication in TRT-HU1 cells stimulated with IL-1β evaluated by Lucifer yellow (LY) microinjection. Image from one representative experiment with and without IL-1β stimulation (green, LY; blue, Hoechst 33342), and dye spread quantification within the region of interest (ROI) (n = 19 each; average cell number in ROIs was 42.2 ± 2.1 and 44.5 ± 4.0, respectively; mean ± SEM). *** $P < 0.0001$ by unpaired *t*-test. Scale bar = 100 μm. For relative levels, values of *Panx1*$^{+/+}$ naïve mice in (A) and time 0 h in (B) and (C) were set as 1. All error bars represent SEM.

MAPK with SB203580 but not of ERK with U0126 completely blocked Cx43 upregulation induced by IL-1β stimulation (Figure 5B). This inhibition of p38 MAPK was accompanied by decrease of STAT1 phosphorylation (Supplementary Fig. S9). Fludarabine, an antitumor genotoxic agent and also an activator of STAT1 in p53-expressing cells[42], further enhanced IL-1β induced Cx43 upregulation, which was completely blocked by SB203580 (Figure 5B). These results indicate that Cx43 upregulation induced by IL-1β is mediated by p38 MAPK and potentiated by the STAT1 signaling pathway.

Next, we examined whether in TRT-HU1 cells the IL-1β - p38 MAPK - STAT1 pathways could also regulate *IL-1β* and *IL-1R-1* mRNA expression, as reported in previous studies showing that IL-1β increased *IL-1β* and *IL-1R-1* mRNA levels[43,44]. Indeed, the expression of *IL-1β, IL-1R-1* and also *STAT1* mRNA levels were significantly upregulated in TRT-HU1 cells following IL-1β stimulation (Figure 5C). The IL-1β induced upregulation of these genes was also inhibited by SB203580 and potentiated by Fludarabine (Figure 5D).

Upregulation of pannexin 1 and caspase-1 by IL-1β stimulation. Since significant upregulation of *IL-1β* and *IL-1R-1* mRNA levels were detected in *Panx1*$^{+/+}$ EAE mice but not in *Panx1*$^{-/-}$ EAE

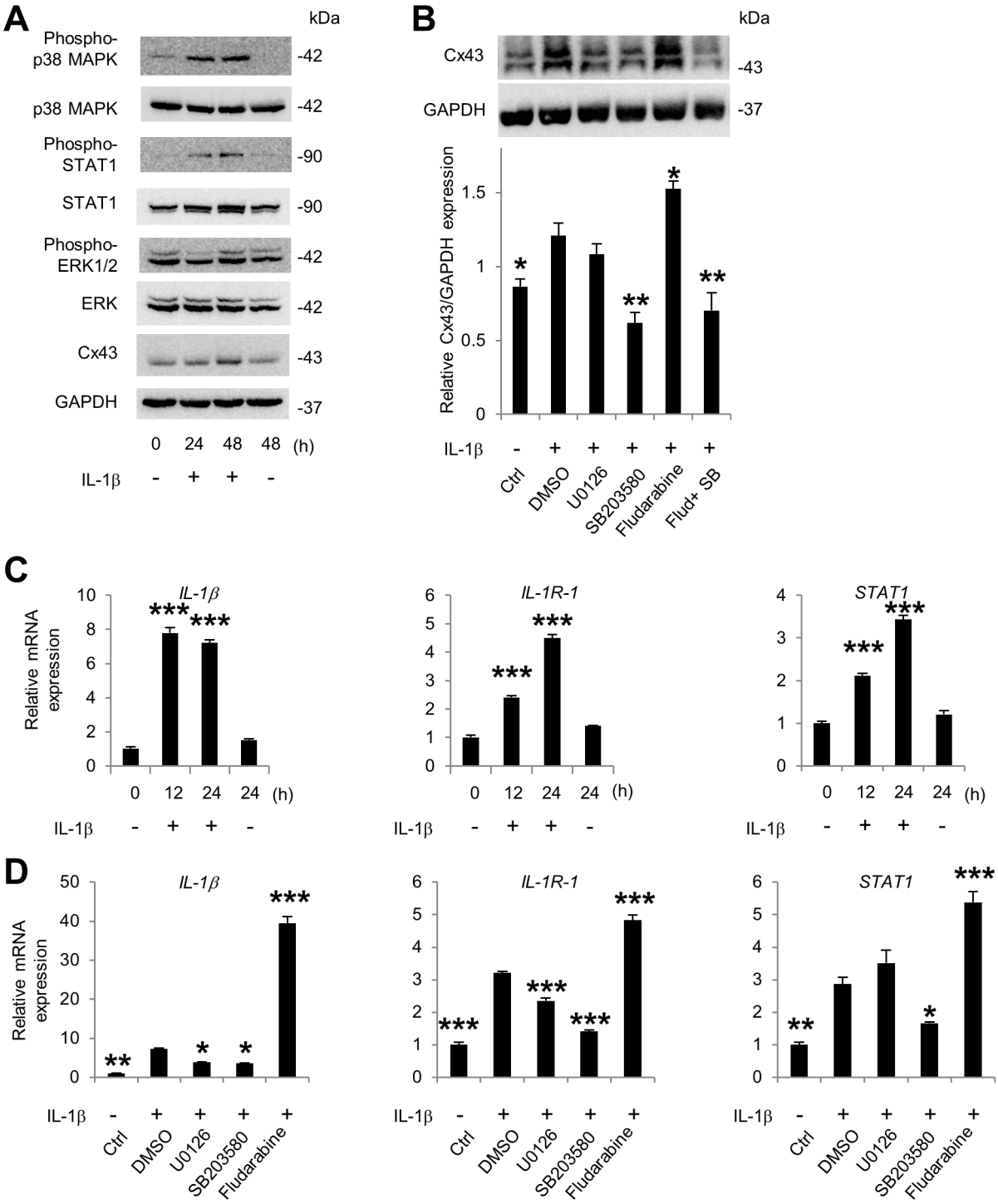

Figure 5 | IL-1β signaling via p38 MAPK. (A) IL-1β increased phosphorylation of p38 MAPK and STAT1 but not of ERK (full-length blots are presented in Supplementary Fig. S14). (B) IL-1β induced upregulation of Cx43 expression was blocked by SB203580 but not U0126 and was potentiated by Fludarabine treatment at 48 h (full-length blots are presented in Supplementary Fig. S14). * $P < 0.05$ and ** $P < 0.01$ compared with DMSO by one-way ANOVA followed by Dunnett's *post hoc* test. (C, D) IL-1β stimulation increased *IL-1β*, *IL-1R-1* and *STAT1* mRNA levels in TRT-HU1 cells in (C), a response that was blocked by SB203580 and enhanced by Fludarabine in (D) at 24 h. *** $P < 0.0005$ compared with time 0 h and 24 h without IL-1β by one-way ANOVA followed by Tukey's *post hoc* test in (C) (n = 3). * $P < 0.05$, ** $P < 0.01$ and *** $P < 0.0005$ compared with DMSO by one-way ANOVA followed by Dunnett's *post hoc* test in (D) (n = 3). All error bars indicate SEM.

mice during the chronic phase (Figure 4A), and because Panx1 signaling is required for caspase-1 activation[45], we hypothesized that pannexin 1 could be involved in this positive feedback loop. Stimulation of TRT-HU1 cells with IL-1β increased *PANX1* mRNA expression level after 12 h (Figure 6A) and increased protein levels at 12 h and 24 h (Figure 6B; differences in pattern and size of pannexin 1 bands detected in bladder tissues (Fig. 2) and TRT-HU1 cells may be due to either species difference, to the use of tissue and cultured cells or to levels of Panx1 glycosylation[46]). In addition, expression of *CASP1* mRNA was also upregulated at 12 h and 24 h (Figure 6C, left panel) after IL-1β stimulation. *CASP1* upregulation at 12 h was inhibited by mefloquine (MFQ), a

Panx1 channel blocker (Figure 6C, right panel). CASP1 upregulation by IL-1β stimulation and the inhibitory effect of MFQ were confirmed on the protein level by immunoblotting (Figure 6D).

These findings indicate that Panx1 channels are involved in the IL-1β positive feedback loop via caspase-1 activation in TRT-HU1 cells.

Blockade of pannexin 1 signaling inhibits Cx43 upregulation by IL-1β stimulation. Finally, we evaluated whether pharmacological blockade of Panx1 channels could prevent Cx43 upregulation following IL-1β stimulation. Upregulation of *Cx43* mRNA and its protein in TRT-HU1 cells induced by IL-1β stimulation was prevented by MFQ treatment (Figures 7A and B). This MFQ effect was accompanied by a decrease in p38 MAPK and STAT1 phosphorylation but without altering the phosphorylation state of ERK.

Therefore, we propose the presence in urothelial cells of a positive feedback loop involving Panx1 and IL-1β signaling pathways via caspase-1 and IL-1R-1 that modulates Cx43 expression through p38 MAPK and STAT1 (Figure 7C).

Discussion

Bladder dysfunction is common in MS patients and symptoms include low compliance and hypersensitivity leading to insufficient urine storage, excretion and incontinence. Detrusor sphincter dyssynergia (DSD) is a characteristic condition that causes high pressure voiding in MS patients as well as in spinal cord injured patients. These conditions are mainly treated palliatively with pharmacological approaches such as treatment with anticholinergics and neuromodulators, depending on major symptoms and urodynamic findings. When all other possible managements fail, indwelling catheter is recommended and is applied in approximately 30% of MS patients[47]. Further advances in preventing and treating this bothersome situation would certainly be expected to improve the quality of life of MS patients.

In this study we showed that in mice with EAE, an animal model of MS, genetic depletion of *Panx1* ameliorated micturition function and prevented the upregulation of *IL-1β* and *Cx43* in bladder mucosa seen in EAE mice. We also disclosed a mechanism that is likely involved in these alterations, comprising a positive feedback loop between Panx1 and IL-1β signaling pathways via Casp1 and IL-1R-1 that modulates Cx43 expression in urothelial cells.

Our results with EAE mice showing insufficient voiding under free-moving condition and increased bladder weight are consistent with previous reports[5–7]. Interestingly, however, bladder dysfunction was not correlated with the severity of EAE in acute phase. For instance, in the acute phase of EAE, even when the neurological score was as high as 2.5, with animals showing severe hindlimb paresis, micturition dysfunction was not evident, despite changes in expression of several genes associated with the bladder mechanosensory, transduction and signaling systems. In contrast, in the chronic phase of the disease, micturition dysfunction was prevalent. This progression to micturition dysfunction could be due to unknown initial compensatory mechanisms or to the natural temporal progression of the disease. Compensatory mechanisms have been proposed to

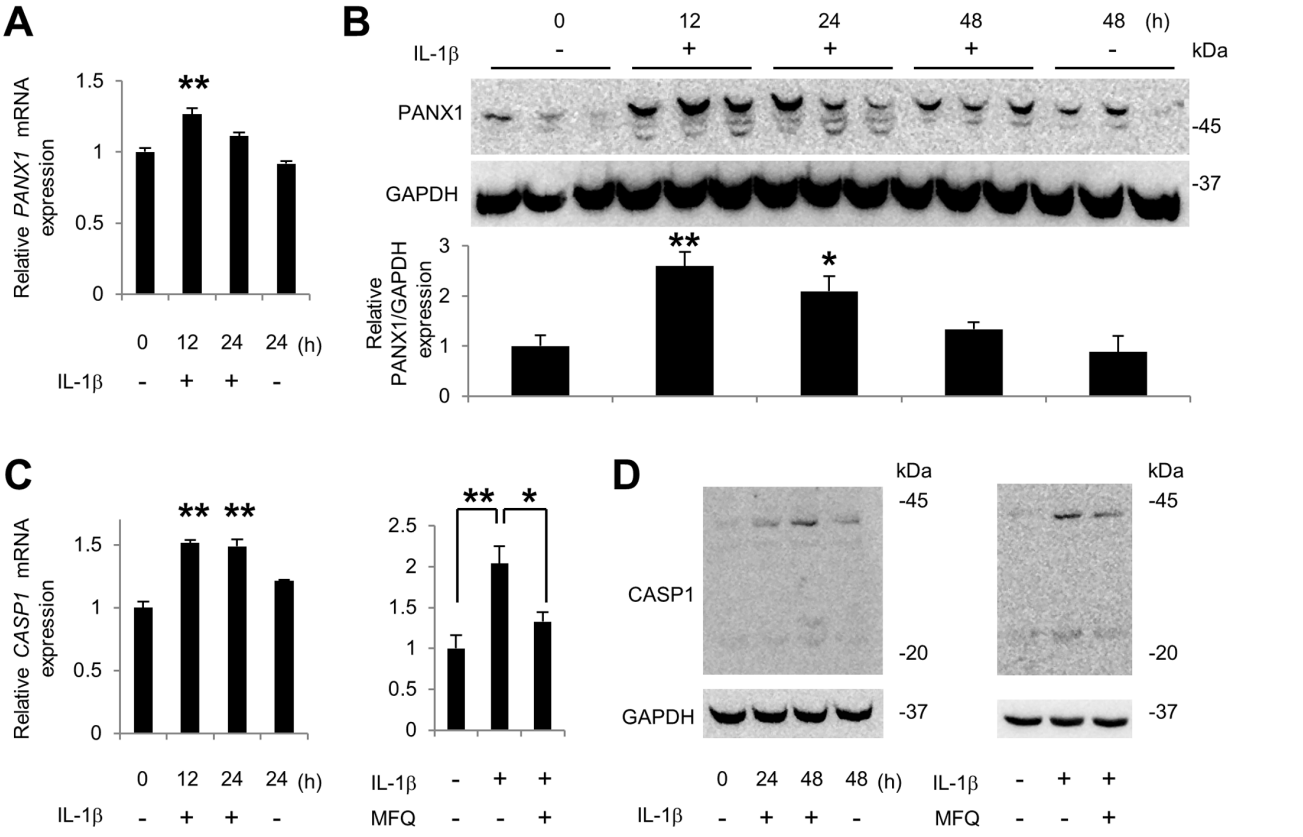

Figure 6 | IL-1β stimulation increases pannexin 1 and caspase-1 expression in urothelial cells. (A, B) IL-1β stimulation of TRT-HU1 cells increased levels of *Panx1* mRNA in (A) and its protein in (B) (full-length blots are presented in Supplementary Fig. S15). ** $P < 0.01$ and * $P < 0.05$ compared with time 0 and 24 in (A) or 48 in (B) without IL-1β by one-way ANOVA followed by Tukey's *post hoc* test (n = 3). (C, D) IL-1β stimulation of TRT-HU1 cells increased levels of *CASP1* mRNA in (C) and its protein in (D), a response that was inhibited by the Panx1 channel blocker mefloquine (MFQ) at 24 h in (C) and at 48 h in (D) (full-length blots are presented in Supplementary Fig. S15). ** $P < 0.01$ compared with time 0 and 24 without IL-1β by one-way ANOVA followed by Tukey's *post hoc* test in (C), left panel (n = 3). * $P < 0.05$ and ** $P < 0.01$ by one-way ANOVA followed by Dunnett's *post hoc* test in (C), right panel (n = 3). All error bars indicate SEM.

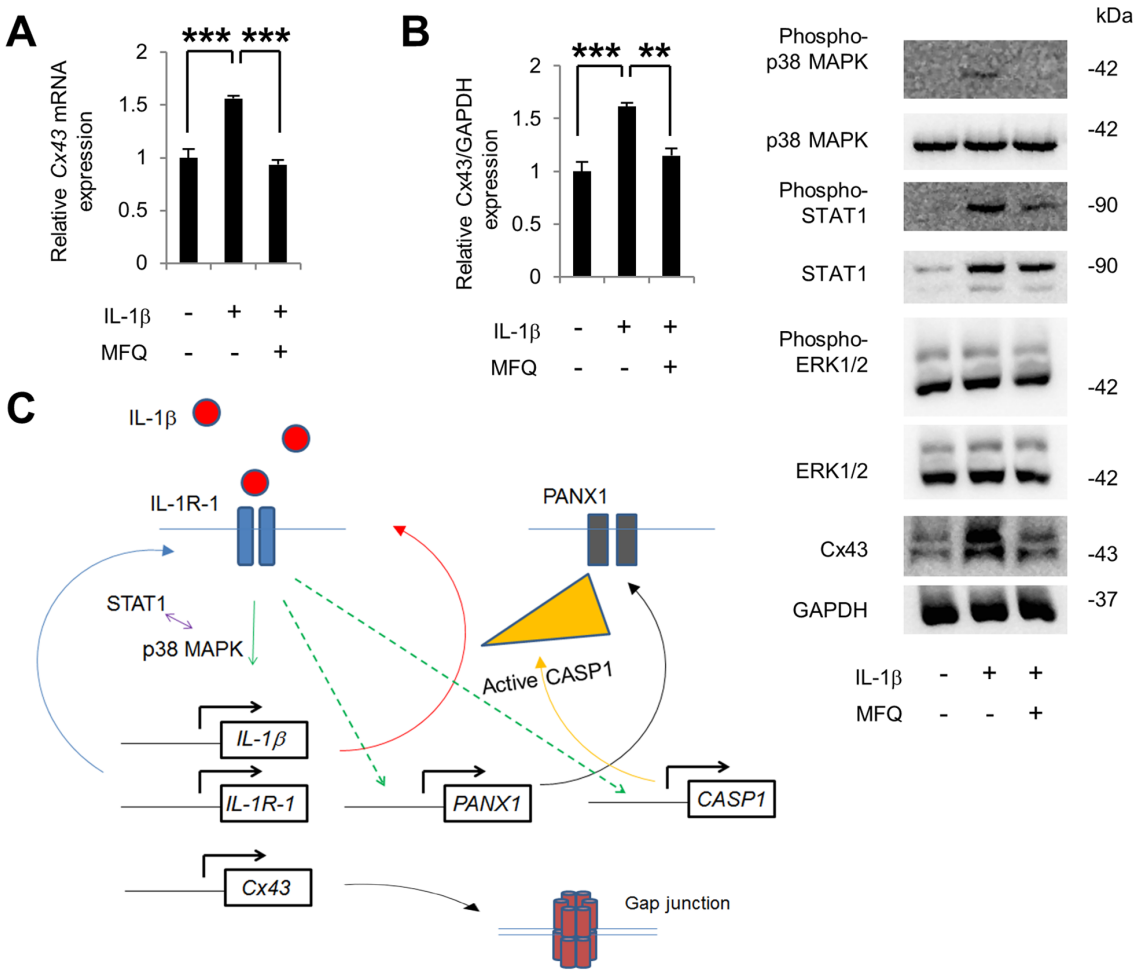

Figure 7 | Mefloquine inhibits IL-1β induced Cx43 upregulation. (A, B) Treatment of TRT-HU1 cells with mefloquine (MFQ) inhibited IL-1β induced increase of *Cx43* mRNA in (A) and its protein in (B), an event that was accompanied by decreased phosphorylation of p38 MAPK and STAT1 but not of ERK (full-length blots are presented in Supplementary Fig. S16). *** $P < 0.0001$ by one-way ANOVA followed by Dunnett's *post hoc* test in (A) (n = 3), and *** $P < 0.005$ and ** $P < 0.01$ by one-way ANOVA followed by Dunnett's *post hoc* test in (B) (n = 3). All error bars indicate SEM. (C) A putative mechanism for Panx1 regulation of Cx43 expression through a positive feedback loop with IL-1β signaling. IL-1R-1 stimulation by IL-1β increases Cx43 expression and upregulates *IL-1β and IL-1R-1* via p38 MAPK and STAT1 activation; through a still unknown pathway, IL-1R-1 stimulation also upregulates *PANX1* and *CASP1*. In turn, PANX1 signaling activates CASP1, which results in maturation of IL-1β thereby closing the functional loop between PANX1 and IL-1β that regulates Cx43 expression.

account for the initial maintenance of bladder function in other disease states, such as in the early phase of the partial bladder outlet obstruction model[48], but their actual nature is still unclear.

Because *Panx1* and *Cx43* mRNA expression levels were upregulated in both acute and chronic phases of EAE, we investigated the mechanism by which these two gap junctions were regulated. For that we first manipulated *Panx1* gene expression to investigate its contribution to bladder dysfunction that emerges in the chronic phase. A major finding of this study is that $Panx1^{-/-}$ EAE mice have lesser micturition dysfunction when compared to $Panx1^{+/+}$ EAE mice. Use of bladder specific *Panx1* knockout mice would be the most attractive method for clarifying the contribution of Panx1 in EAE-related bladder complications, but such mice have not yet been generated. Nonetheless, because $Panx1^{-/-}$ EAE mice developed as severe neurological symptoms as $Panx1^{+/+}$ EAE mice, it can be assumed that depletion of Panx1 expression in the bladder rather than in the CNS play a role in the amelioration of micturition function in EAE mice. In addition, the fact that genes such as *P2ry1* and *Chrm2* in the mucosa, and *P2ry2* and *P2ry6* in the detrusor were similarly regulated in both $Panx1^{+/+}$ EAE and $Panx1^{-/-}$ EAE mice suggests that these genes are not associated with amelioration of bladder function in $Panx1^{-/-}$ EAE mice. On the other hand, because others genes such as *Trpv4* in the mucosa and *Col1a1* and *Ctgf1* in the detrusor were differentially regulated in the two genotypes, it is possible that they may contribute, to a certain extent, to ameliorate bladder function in $Panx1^{-/-}$ EAE mice when compared to their wild type counterparts.

Notably, our observation that Cx43 upregulation in the bladder mucosa of EAE mice was prevented in $Panx1^{-/-}$ EAE mice suggest that Panx1 maybe upstream of a signaling cascade that regulates Cx43 expression. Lamina propria myofibroblasts express Cx43, and coupling through Cx43 gap junctions has been proposed to mediate intercellular signaling and coordination of cellular activity within and between the bladder mucosa and detrusor muscle. The role of Cx43 in urothelium has been mainly investigated under pathological conditions, as in urothelial carcinoma[49,50], but little is still known about urothelial Cx43 function in a physiological setting. Gap junctions formed by Cx43 are permeable to Lucifer Yellow (LY) while those formed by Cx26, another gap junction protein in urothelium, are less permeable to this dye[51]. In our studies with TRT-HU1 cells, LY dye spread was more extensive among cells stimulated with IL-1β, which concurred with increased Cx43 expression in these urothelial cells and with our previous report that $Cx43^{+/-}$ mice have higher UVVM than $Cx43^{+/+}$ mice[29], indicating that gap junctions

formed by Cx43 may have an important role in transmission and coordination of signals within the urothelium. Besides forming gap junction channels, non-apposed Cx43 hemichannels (connexons) have been proposed to open in certain conditions and provide a conduit for exchange of small ions and molecules between the intracellular compartment and extracellular milieu (reviewed in[25]). While in this study we demonstrated that Cx43 functions as a gap junction channel in urothelial cells and that increased intercellular coupling likely plays a major role in EAE bladder dysfunction, we have not addressed whether Cx43 hemichannels could also contribute. The role of hemichannels deserves to be investigated in future studies.

Our present study with urothelial cells also disclosed a putative molecular mechanism for Panx1-mediated regulation of Cx43 expression involving a functional interplay between Panx1 and IL-1β signaling. We found that IL-1β upregulates *PANX1* expression, and through IL-1R-1 via p38 MAPK and also STAT1, IL-1β upregulates its own transcription and that of *IL-1R-1* and *Cx43*. Given that maturation of IL-1β requires the activated form of caspase-1, which has been shown to involve Panx1 signaling[26], a positive feedback loop involving Panx1 and IL-1β would thereby be generated, through which Panx1 signaling would modulate Cx43 expression in the urothelium. Besides this proposed modulation of Cx43 expression at the transcriptional level, other Cx43 regulatory mechanisms could also be involved. IL-1β and other cytokines are known to modulate internal ribosome entry site (IRES) mediated translation (for example[52]). It has been shown that *Cx43* mRNA contains a functional IRES element[53] and IRES-mediated translation has been proposed as an alternative mechanism for rapid regulation of Cx43 protein expression without requiring de novo mRNA synthesis (reviewed in[54]). However, demonstration that IL-1β regulates Cx43 expression via an IRES-dependent mechanism still needs to be provided.

Our findings that pharmacological blockade of Panx1 channels and of p38 MAPK inhibited Cx43 upregulation by IL-1β stimulation in urothelial cells suggest that such intervention could be potentially used as a novel therapeutic approach to prevent and treat bladder dysfunction in EAE/MS. Fludarabine, a STAT1 inducer in p53-expressing cells, significantly increased the expression of genes involved in this loop, which implies that other simultaneous stimulation to urothelial cells involving STAT1 activation could potentiate the response to IL-1β. STAT1 is a member of JAK/STAT pathway and is required for the cellular response to interferons[55]. STAT1 is also reported to have important role for activating caspase-1 and IL-1β release[56]. In such cases, prevention of inflammatory response in the bladder may be beneficial. Although it is still unclear which events in EAE would trigger the inflammatory response in the bladder, such response is not likely associated with macrophages. We observed that the mRNA levels of EGF-like module containing, mucin-like, hormone receptor-like sequence 1 (*Emr1*, a marker of macrophage)[57] and tumor necrosis factor alpha (*Tnfa*) were not significantly upregulated in bladder of EAE mice in both acute phase and chronic phase (Supplementary Figs. S8 and S10). It has been speculated that circulating toxic factors cause bladder dysfunction in MS patients[1]. Of note is the fact that IL-1β is upstream of the cytokine signaling cascade[58] and, in this case, the proposed Panx1-IL-1β functional loop may have influenced other inflammatory pathways in MS/EAE. This possibility is supported by our findings that upregulation of *IL-6* and *NF-kappaB1* (*Nfkb1*, a critical regulator of inflammation) mRNA levels in mucosa was remarkably decreased in *Panx1*$^{-/-}$ EAE (Supplementary Fig. S8).

In summary, we show here that micturition dysfunction in EAE mice is associated with changes in expression of key molecular mediators of the bladder intrinsic mechanosensory, transduction and signaling systems. We propose that one of the mechanisms underlying such remodeling of the bladder in EAE involves a positive feedback loop between Panx1 and IL-1β signaling via Casp1 and IL-1R-1, which modulates Cx43 expression in urothelial cells. This mechanism warrants further translational and clinical approaches, where manipulation of components of this Panx1-IL-1β loop in the bladder may provide a novel therapeutic approach for management of bladder dysfunction in patients with MS.

Methods

Animals. Heterozygous Panx1$^{tm1a(KOMP)Wtsi}$ mice were purchased from the Knockout Mouse Project (KOMP) at UCDavis and bred at the Albert Einstein College of Medicine (AECOM) facilities to obtain homozygous mice for the transgene (*Panx1*$^{-/-}$), heterozygous (*Panx1*$^{+/-}$) and wild type (*Panx1*$^{+/+}$). Fetus of *Cx43* knockout (*Cx43*$^{-/-}$), heterozygote (*Cx43*$^{+/-}$) and wild type littermates (*Cx43*$^{+/+}$) were obtained from cesarean section of full term *Cx43*$^{+/-}$ mice (heterozygous C57BL/6J-Gja1^{tm1Kdr}, Jackson Laboratory) maintained at AECOM. Wild type C57BL/6 mice at 8 weeks old were purchased from the Jackson laboratory (Bar Harbor, Maine, USA). Animals were treated in accordance with NIH animal care guidelines, and the AECOM Animal Experiment Committee approved all animal experiments.

Induction of experimental autoimmune encephalomyelitis (EAE). EAE was induced in C57BL/6 wild type, *Panx1*$^{+/+}$ and *Panx1*$^{-/-}$ mice by subcutaneous immunization with 300 μg of myelin oligodendrocyte glycoprotein MOG_{35-55} peptide (MEVGWYRSPFSRVVHLYRNGK; Celtek Bioscience, Nashville, TN, USA) in a 200 μl emulsion composed of equal parts of MOG and Incomplete Freund's Adjuvant (DIFCO Laboratories, Detroit, MI, USA) supplemented with heat-killed *Mycobacterium tuberculosis* H37Ra (DIFCO Laboratories) at 10 mg/mL. The day of MOG immunization was designated day 0. On day 0 and day 2 post immunization (dpi), mice were injected intraperitoneally with 500 ng Pertussis toxin (List Biological Laboratories, Campbell, CA, USA). As control, CFA (Complete Freund's Adjuvant) without MOG was used. Clinical signs of disease were scored in a 0–5 scale: 0, No clinical signs; 0.5, partially limp tail; 1, paralyzed tail; 1.5, mild hind limb paresis; 2, loss in coordinated movement or hind limb paresis; 2.5, sever hind limb paresis or one hind limb paralyzed; 3, both hind limbs paralyzed; 3.5, hind limbs paralyzed or weakness in forelimbs; 4, forelimbs paralyzed; 5, moribund. To compare *Panx1*$^{+/+}$ and *Panx1*$^{-/-}$ mice with EAE, mice with similar clinical scores with not less than 1.5 were used.

Micturition analysis in mice. The automated Voided Stain on Paper (aVSOP) method was used in this study, which is a micturition recording system for mice that was previously described by us[29,30]. Briefly, rolled laminated filter paper that turn deep purple at the edge of urine stains, was wound up at a speed of 10 cm/h under a water-repellant wire lattice. Urine stains were counted, traced, the area calculated and converted to micturition volume using a standard curve. Mice were individually kept in cages with 75 × 160 × 75 mm (height × depth × width), with free access to water and food, and maintained under 12-hour light/dark cycle. Micturitions measurements were performed for one day on 4 control naïve C57BL/6 mice, 3 mice with EAE (acute phase) and 6 mice with EAE (chronic phase). For some experiments micturition was followed for 4 days in 3 *Panx1*$^{+/+}$ and 3 *Panx1*$^{-/-}$ naïve mice and for one day in 3 *Panx1*$^{+/+}$ EAE and 8 *Panx1*$^{-/-}$ EAE.

Cell culture. The hTERT-immortalized human urothelial cell line (TRT-HU1), generated by Dr. Louis S. Liou[37] and kindly provided by Dr. Rosalyn M. Adam (Urological Diseases Research Center, Children's Hospital Boston, Boston), were maintained in DMEM (GIBCO, Life Technologies, Grand Island, NY) containing 2 mM L-glutamine and 110 mg/L sodium pyruvate supplemented with 15% fetal bovine serum (FBS, GIBCO), non-essential amino acids (GIBCO), and 1.15 mM 1-thioglycerol, as previously described[37].

IL-1β stimulation. Confluent cultures of TRT-HU1 cells were stimulated with 2 ng/ml IL-1β (Peprotech, Rocky Hill, NJ, USA) after two days in urothelial medium containing 0.5% FBS. In some experiments, 10 μM U0126 [Cell Signaling Technology (CST)], 10 μM SB203580 (CST), 50 μM Fludarabine (TOCRIS bioscience) and 100 nM mefloquine (MFQ; QU024-1, BioBlocks, San Diego, CA, USA) were added 2 hour, 2 hour, 24 hour and 15 minutes, respectively, prior to IL-1β stimulation.

Real-time RT-PCR. Complementary DNA was synthesized from 1 μg of RNA extracted from the bladder mucosa and detrusor muscle tissue, and from cultured TRT-HU1 cells using a Superscript VILO cDNA Synthesis Kit (Invitrogen, Life Technologies, Grand Island, NY, USA). Primers used are listed in **Supplementary Table S1**. Real-time RT-PCR was performed using SYBR Green PCR Master Mix (Applied Biosystems, Life Technologies) with 7300 Fast Real-Time PCR system (Applied Biosystems, Life Technologies). Reaction mixtures were denatured at 95°C for 10 min, followed by 40 PCR cycles. Each cycle consisted of following three steps: 94°C for 15 s, 57°C for 15 s, and 72°C for 1 min. Each sample was normalized against an internal 18 s ribosomal RNA control.

Immunoblotting. Bladder mucosa was gently separated from the detrusor muscle using fine tweezers and a dissecting microscope. Whole cell lysates from bladder mucosa and cultured TRT-HU1 cells were lysed with sample buffer (1 mM $NaHCO_3$, 2 mM phenylmethylsulphonyl fluoride, 1 mM Na_3VO_4, 5 mM EDTA and 1% Triton

X-100) containing proteinase inhibitors (Roche laboratories, Basle, Switzerland)[33], which were resolved by SDS-PAGE and transferred to a nitrocellulose membrane (Whatman, Dassel, Germany). After 30 min incubation with blocking buffer containing 0.5% Tween-20 (TBS-T) and 5% nonfat dry milk, at room temperature, the membranes were incubated for over-night at 4°C with antibodies against Cx43 (polyclonal 1 : 1000; Sigma-Aldrich, St. Louis, MO, USA), Panx1 (N-terminal 1 : 100; Invitrogen), GAPDH (1 : 2000; Fitzgerald, Acton, MA, USA), phospho-p38 MAPK (1 : 1000; CST), p38 MAPK (1 : 1000; CST), pY701 phospho-STAT1 (1 : 500; Biosource, Life Technologies), STAT1 (1 : 250; BD Transduction Laboratories, Franklin Lakes, NJ, USA), phospho-ERK (1 : 1000; CST), ERK (1 : 1000; CST) and caspase-1 (1 : 1000; Millipore, Billerica, MA, USA). After several washes with TBS-T, the membranes were incubated with HRP-conjugated anti-rabbit or mouse IgG antibody (Santa Cruz Biotechnology, Santa Cruz, CA, USA) for 1 h at room temperature. Immunoreactive bands were then visualized using the Kodak Imaging station (Care-stream Health, Rochester, NY, USA) following the incubation of the membranes with enhanced chemiluminescence reagents (Millipore). Images obtained were analyzed using ImageJ 1.46 r software (NIH) using GAPDH as an invariant control against which the protein of interest was normalized.

Immunostaining of the urinary bladder. Mice bladder tissues were fixed with 4% paraformaldehyde at 4°C over-night, followed by cryoprotection at 4°C in 10%, 20% and then 30% sucrose for equal periods of 24 hr. The bladder tissues were then embedded in Tissue-TEK OCT compound (Sakura, Torrance, CA, USA), frozen in liquid nitrogen, and 5 μm thick sections were cut with a microtome. After permeabilization with 0.25% Triton X-100 and block with 10% goat serum (Invitrogen), sections were incubated with Cx43 rabbit polyclonal antibody (1 : 500; Sigma-Aldrich). Immunoreactivity was visualized using goat anti-rabbit Alexa Fluor 594 (Molecular Probes, Invitrogen), and counter stained with DAPI. Images were acquired using a Nikon Eclipse TE300 microscope equipped with FITC, Texas red and DAPI filter sets and a SPOT-RT digital camera (Diagnostic Instruments, Sterling Heights, MI, USA).

Immunostaining of urothelium explants. Primary urothelial cells grown from explants of bladder mucosa isolated from full term *Cx43*$^{-/-}$, *Cx43*$^{+/-}$ and *Cx43*$^{+/+}$ foetuses were cultured on 50 mm glass bottomed dishes (MatTek Corporation, Ashland, MA, USA) and maintained in urothelial medium. Cells were fixed with 4% paraformaldehyde in PBS at 4°C, permeabilized with 0.4% Triton X-100, and blocked with 10% goat serum (Invitrogen). The samples were incubated with Cx43 rabbit polyclonal antibody (1 : 500; Sigma-Aldrich) and E-cadherin mouse monoclonal antibody (1 : 250; BD Transduction,) followed by goat anti-rabbit Alexa 594 and anti-mouse Alexa 488 (Molecular Probes) and counter stained with DAPI.

Lucifer yellow microinjections. TRT-HU1 cells were live stained with 16 μM of Hoechst 33342 (Invitrogen) for 15 minutes to facilitate visualization and quantification of number of cells per injected region of interest (ROI), and Lucifer yellow (LY) microinjected as previously described[29]. Briefly, a single cell was impaled with a microelectrode and LY iontophoretically injected for 3 minutes with a continuous current of 0.1 μA using an electrometer (model 3100; A-M systems). Images were acquired with a CoolSNAP-HQ2 CCD camera (Photometrics) attached to an inverted microscope. LY fluorescent cells within the ROI were counted and the values were normalized to the total number of cells in the ROI.

Statistical analysis. For the micturition experiments, data was analyzed using Kruskal Wallis test followed by Dunn's *post-hoc* test to compare three groups. Two-way repeated measures ANOVA was used to compare differences between clinical index of *Panx1*$^{+/+}$ mice and *Panx1*$^{-/-}$ mice with EAE. For the experiments in which three or more test groups were compared, we used one-way ANOVA followed by Tukey's *post hoc* test. For analysis of qPCR experiments of *Panx1*$^{+/+}$ mice and *Panx1*$^{-/-}$ mice with and without EAE, we used one-way ANOVA followed by Bonferroni's *post hoc* test set the 4 comparisons as naïve *Panx1*$^{+/+}$ mice vs. naïve *Panx1*$^{-/-}$ mice, naïve *Panx1*$^{+/+}$ mice vs. EAE *Panx1*$^{+/+}$ mice, naïve *Panx1*$^{-/-}$ mice vs. EAE *Panx1*$^{-/-}$ mice, and EAE *Panx1*$^{+/+}$ mice vs. EAE *Panx1*$^{-/-}$ mice.

1. McCombe, P. A., Gordon, T. P. & Jackson, M. W. Bladder dysfunction in multiple sclerosis. *Expert Rev. Neurother.* **9**, 331–340 (2009).
2. de Seze, M., Ruffion, A., Denys, P., Joseph, P. A. & Perrouin-Verbe, B. The neurogenic bladder in multiple sclerosis: review of the literature and proposal of management guidelines. *Mult. Scler.* **13**, 915–928 (2007).
3. Lassmann, H. Models of multiple sclerosis: new insights into pathophysiology and repair. *Curr. Opin. Neurol.* **21**, 242–247 (2008).
4. Constantinescu, C. S., Farooqi, N., O'Brien, K. & Gran, B. Experimental autoimmune encephalomyelitis (EAE) as a model for multiple sclerosis (MS). *Br. J. Pharmacol.* **164**, 1079–1106 (2011).
5. Al-Izki, S., Pryce, G., Giovannoni, G. & Baker, D. Evaluating potential therapies for bladder dysfunction in a mouse model of multiple sclerosis with high-resolution ultrasonography. *Mult. Scler.* **15**, 795–801 (2009).
6. Altuntas, C. Z. *et al.* Bladder dysfunction in mice with experimental autoimmune encephalomyelitis. *J. Neuroimmunol.* **203**, 58–63 (2008).
7. Altuntas, C. Z. *et al.* Connective tissue and its growth factor CTGF distinguish the morphometric and molecular remodeling of the bladder in a model of neurogenic bladder. *Am. J. Physiol. Renal Physiol.* **303**, F1363–F1369 (2012).
8. Vignes, J. R., Deloire, M. S., Petry, K. G. & Nagy, F. Characterization and restoration of altered inhibitory and excitatory control of micturition reflex in experimental autoimmune encephalomyelitis in rats. *J. Physiol.* **578**, 439–450 (2007).
9. Mizusawa, H. *et al.* A rat model for investigation of bladder dysfunction associated with demyelinating disease resembling multiple sclerosis. *Neurourol. Urodyn.* **19**, 689–699 (2000).
10. Ciancio, S. J., Mutchnik, S. E., Rivera, V. M. & Boone, T. B. Urodynamic pattern changes in multiple sclerosis. *Urology* **57**, 239–245 (2001).
11. Andersson, K. E. & Arner, A. Urinary bladder contraction and relaxation: physiology and pathophysiology. *Physiol. Rev.* **84**, 935–986 (2004).
12. Birder, L. A. & de Groat, W. C. Mechanisms of disease: involvement of the urothelium in bladder dysfunction. *Nat. Clin. Pract. Urol.* **4**, 46–54 (2007).
13. Davidoff, R., Yamaguchi, R., Leach, G. E., Park, E. & Lad, P. M. Multiple urinary cytokine levels of bacterial cystitis. *J. Urol.* **157**, 1980–1985 (1997).
14. Imamura, M. *et al.* Basic fibroblast growth factor modulates proliferation and collagen expression in urinary bladder smooth muscle cells. *Am. J. Physiol. Renal Physiol.* **293**, F1007–F1017 (2007).
15. Dozmorov, M. G. *et al.* Systems biology approach for mapping the response of human urothelial cells to infection by Enterococcus faecalis. *BMC Bioinformatics 8 Suppl* **7**, S2 (2007).
16. Wognum, S., Lagoa, C. E., Nagatomi, J., Sacks, M. S. & Vodovotz, Y. An exploratory pathways analysis of temporal changes induced by spinal cord injury in the rat bladder wall: insights on remodeling and inflammation. *PLoS One* **4**, e5852 (2009).
17. Imamura, M. *et al.* Basic fibroblast growth factor causes urinary bladder overactivity through gap junction generation in the smooth muscle. *Am. J. Physiol. Renal Physiol.* **297**, F46–F54 (2009).
18. Negoro, H. *et al.* Regulation of connexin 43 by basic fibroblast growth factor in the bladder: transcriptional and behavioral implications. *J. Urol.* **185**, 2398–2404 (2011).
19. Birder, L. A. Nervous network for lower urinary tract function. *Int. J. Urol.* **20**, 4–12 (2013).
20. Roosen, A. *et al.* A refocus on the bladder as the originator of storage lower urinary tract symptoms: a systematic review of the latest literature. *Eur. Urol.* **56**, 810–819 (2009).
21. Ford, A. P. & Cockayne, D. A. ATP and P2X purinoceptors in urinary tract disorders. *Handb. Exp. Pharmacol.* **202**, 485–526 (2011).
22. Nile, C. J. & Gillespie, J. I. Interactions between cholinergic and prostaglandin signaling elements in the urothelium: role for muscarinic type 2 receptors. *Urology* **79**, 240.e17–240.e23 (2012).
23. Skryma, R., Prevarskaya, N., Gkika, D. & Shuba, Y. From urgency to frequency: facts and controversies of TRPs in the lower urinary tract. *Nat. Rev. Urol.* **8**, 617–630 (2011).
24. Fry, C. H., Sui, G. P., Kanai, A. J. & Wu, C. The function of suburothelial myofibroblasts in the bladder. *Neurourol. Urodyn.* **26**, 914–919 (2007).
25. Scemes, E., Spray, D. C. & Meda, P. Connexins, pannexins, innexins: novel roles of "hemi-channels". *Pflugers Arch.* **457**, 1207–1226 (2009).
26. Silverman, W. R. *et al.* The pannexin 1 channel activates the inflammasome in neurons and astrocytes. *J. Biol. Chem.* **284**, 18143–18151 (2009).
27. Gulbransen, B. D. *et al.* Activation of neuronal P2X7 receptor-pannexin-1 mediates death of enteric neurons during colitis. *Nat. Med.* **18**, 600–604 (2012).
28. Thi, M. M., Islam, S., Suadicani, S. O. & Spray, D. C. Connexin43 and pannexin1 channels in osteoblasts: who is the "hemichannel"? *J. Membr. Biol.* **245**, 401–409 (2012).
29. Negoro, H. *et al.* Involvement of urinary bladder Connexin43 and the circadian clock in coordination of diurnal micturition rhythm. *Nat. Commun.* **3**, 809 (2012).
30. Negoro, H. *et al.* Development of diurnal micturition pattern in mice after weaning. *J. Urol.* **189**, 740–746 (2013).
31. Kim, J. E. & Kang, T. C. The P2X7 receptor-pannexin-1 complex decreases muscarinic acetylcholine receptor-mediated seizure susceptibility in mice. *J. Clin. Invest.* **121**, 2037–2047 (2011).
32. Csak, T. *et al.* Fatty acid and endotoxin activate inflammasomes in mouse hepatocytes that release danger signals to stimulate immune cells. *Hepatology* **54**, 133–144 (2011).
33. Suadicani, S. O., Urban-Maldonado, M., Tar, M. T., Melman, A. & Spray, D. C. Effects of ageing and streptozotocin-induced diabetes on connexin43 and P2 purinoceptor expression in the rat corpora cavernosa and urinary bladder. *BJU Int.* **103**, 1686–1693 (2009).
34. Pelegrin, P. & Surprenant, A. Pannexin-1 couples to maitotoxin- and nigericin-induced interleukin-1beta release through a dye uptake-independent pathway. *J. Biol. Chem.* **282**, 2386–2394 (2007).
35. Li, K. *et al.* Reciprocal regulation between proinflammatory cytokine-induced inducible NO synthase (iNOS) and connexin43 in bladder smooth muscle cells. *J. Biol. Chem.* **286**, 41552–41562 (2011).
36. Tonon, R. & D'Andrea, P. Interleukin-1beta increases the functional expression of connexin 43 in articular chondrocytes: evidence for a Ca2+-dependent mechanism. *J. Bone Miner. Res.* **15**, 1669–1677 (2000).
37. Kim, J. *et al.* An hTERT-immortalized human urothelial cell line that responds to anti-proliferative factor. *In Vitro Cell Dev. Biol. Anim.* **47**, 2–9 (2011).

38. Larsen, C. M. *et al*. Interleukin-1beta-induced rat pancreatic islet nitric oxide synthesis requires both the p38 and extracellular signal-regulated kinase 1/2 mitogen-activated protein kinases. *J. Biol. Chem.* **273**, 15294–15300 (1998).
39. Bellei, B. *et al*. Ultraviolet A induced modulation of gap junctional intercellular communication by P38 MAPK activation in human keratinocytes. *Exp. Dermatol.* **17**, 115–124 (2008).
40. Tsukada, J., Waterman, W. R., Koyama, Y., Webb, A. C. & Auron, P. E. A novel STAT-like factor mediates lipopolysaccharide, interleukin 1 (IL-1), and IL-6 signaling and recognizes a gamma interferon activation site-like element in the IL1B gene. *Mol. Cell. Biol.* **16**, 2183–2194 (1996).
41. Kobierski, L. A., Srivastava, S. & Borsook, D. Systemic lipopolysaccharide and interleukin-1beta activate the interleukin 6: STAT intracellular signaling pathway in neurons of mouse trigeminal ganglion. *Neurosci. Lett.* **281**, 61–64 (2000).
42. Youlyouz-Marfak, I. *et al*. Identification of a novel p53-dependent activation pathway of STAT1 by antitumour genotoxic agents. *Cell Death Differ.* **15**, 376–385 (2008).
43. Warner, S. J., Auger, K. R. & Libby, P. Human interleukin 1 induces interleukin 1 gene expression in human vascular smooth muscle cells. *J. Exp. Med.* **165**, 1316–1331 (1987).
44. Bellehumeur, C., Blanchet, J., Fontaine, J. Y., Bourcier, N. & Akoum, A. Interleukin 1 regulates its own receptors in human endometrial cells via distinct mechanisms. *Hum. Reprod.* **24**, 2193–2204 (2009).
45. Pelegrin, P. & Surprenant, A. Pannexin-1 mediates large pore formation and interleukin-1beta release by the ATP-gated P2X7 receptor. *EMBO J.* **25**, 5071–5082 (2006).
46. Boassa, D. *et al*. Pannexin1 channels contain a glycosylation site that targets the hexamer to the plasma membrane. *J. Biol. Chem.* **282**, 31733–31743 (2007).
47. De Ridder, D. *et al*. Conservative bladder management in advanced multiple sclerosis. *Mult. Scler.* **11**, 694–699 (2005).
48. Buttyan, R., Chen, M. W. & Levin, R. M. Animal models of bladder outlet obstruction and molecular insights into the basis for the development of bladder dysfunction. *Eur. Urol.* **32 Suppl 1**, 32–39 (1997).
49. Lyng, F. M. *et al*. Effect of a tobacco-related nitrosamine on intercellular communication in human urothelial cells: a possible factor in smoking-related bladder carcinogenesis. *Oncol. Res.* **8**, 371–378 (1996).
50. Corteggio, A., Florio, J., Roperto, F. & Borzacchiello, G. Expression of gap junction protein connexin 43 in bovine urinary bladder tumours. *J. Comp. Pathol.* **144**, 86–90 (2011).
51. Kanaporis, G., Brink, P. R. & Valiunas, V. Gap junction permeability: selectivity for anionic and cationic probes. *Am. J. Physiol. Cell Physiol.* **300**, C600–C609 (2011).
52. Rubsamen, D. *et al*. IRES-dependent translation of egr2 is induced under inflammatory conditions. *RNA* **18**, 1910–1920 (2012).
53. Schiavi, A., Hudder, A. & Werner, R. Connexin43 mRNA contains a functional internal ribosome entry site. *FEBS Lett.* **464**, 118–122 (1999).
54. Ul-Hussain, M., Dermietzel, R. & Zoidl, G. Connexins and Cap-independent translation: role of internal ribosome entry sites. *Brain Res.* **1487**, 99–106 (2012).
55. Stark, G. R. & Darnell, J. E. Jr. The JAK-STAT pathway at twenty. *Immunity* **36**, 503–514 (2012).
56. Joshi, V. D. *et al*. A role for Stat1 in the regulation of lipopolysaccharide-induced interleukin-1beta expression. *J. Interferon Cytokine Res.* **26**, 739–747 (2006).
57. Khazen, W. *et al*. Expression of macrophage-selective markers in human and rodent adipocytes. *FEBS Lett.* **579**, 5631–5634 (2005).
58. Basu, A., Krady, J. K. & Levison, S. W. Interleukin-1: a master regulator of neuroinflammation. *J. Neurosci. Res.* **78**, 151–156 (2004).

Acknowledgements

We thank Dr. David C. Spray and Dr. Mia M. Thi for valuable discussions, Marcia Urban-Maldonado, Naman K. Patel and Adriana Mello for technical support and animal care, and Atsumi Negoro for assisting with aVSOP data retrieval. Funding was provided by grants from the National Institutes of Health (DK081435 to SOS, NS52245 to ES and T32 NS07439 to SEL).

Author contributions

H.N. and S.O.S. designed the experiments. H.N. performed most of the experiments and analyzed the data. S.E.L. contributed to EAE induction and clinical scoring. L.S.L. generated TRT-HU1 cells. A.K. and O.O. contributed to aVSOP experiments. H.N., E.S. and S.O.S. wrote the manuscript. All authors reviewed the manuscript.

Additional information

Supplementary information accompanies this paper at http://www.nature.com/scientificreports

Competing financial interests: The authors declare no competing financial interests.

How to cite this article: Negoro, H. *et al*. Pannexin 1 involvement in bladder dysfunction in a multiple sclerosis model. *Sci. Rep.* **3**, 2152; DOI:10.1038/srep02152 (2013).